*IHA Hydrotransport 21 Conference, Edmonton, Canada, 3-5 May 2023*

# Using rotational viscometer test results to predict pipe flow of slurries

*Allan Thomas*
*Slurry Systems Engineering Pty Limited, Australia*

**ABSTRACT**

Turbulent pipe flow involves shear rates far higher than achievable in a rotational bob and cup viscometer, and to extrapolate viscometer data it is argued that the Bingham model is preferable to alternates such as the Herschel-Bulkley model. A method of determining the Bingham parameters is illustrated and a means of predicting the resulting Bingham shear stress-shear rate relationship in the viscometer gap, for both fully sheared and part sheared conditions, is developed. Use of the Bingham model to predict laminar and turbulent flow in pipelines is illustrated. The apparent shear rate 8V/D is shown not appropriate for turbulent flow prediction.

**NOTATION**

| | |
|---|---|
| $C_w$ | Solids concentration by weight, % |
| D | Internal pipe diameter, m |
| h | length of bob, m |
| J | Pressure gradient, Pa/m |
| $k_f$ | Factor given by Eqn 10, - |
| n’ | Slope of logarithmic plot, see Eqn 3, - |
| $R_b$ | Radius of bob, m |
| $R_c$ | Radius of cup, m |
| $R_y$ | Given by Eqn 11 |
| T | Torque measured at bob, Nm |
| V | Velocity in pipe flow, m/s |
| $V_t$ | Laminar/turbulent transition velocity, m/s |
| $\gamma$ | Shear rate, $s^{-1}$ |
| $\gamma_b$ | Shear rate at bob, $s^{-1}$ |
| $\gamma_{crit}$ | Critical shear rate given by Eqn 13 |
| $\eta_{ex}$ | “Plastic” viscosity obtained by fitting a straight line to high shear rate data, Pas |
| $\eta_{pl}$ | Bingham plastic viscosity, Pas |
| $\rho_{sl}$ | Density of slurry, $kg/m^3$ |
| $\tau$ | Shear stress, Pa |
| $\tau_{crit}$ | Critical shear stress given by Eqn 12, Pa |
| $\tau_{ex}$ | Shear stress obtained by extrapolating high shear rate data, Pa |
| $\tau_y$ | Bingham plastic yield stress, Pa |
| $\tau_w$ | Pipe wall shear stress, Pa |
| $\Omega$ | Radial velocity, radians/sec |

# 1 INTRODUCTION

This paper is concerned with design of slurry pipelines to transport slurries with a wide particle size distribution which are fine enough that they have rheological properties which can be measured using a rotational viscometer. Such slurries (concentrates and tailings) are generally the result of grinding of ores, and represent a major portion of all mineral slurries pumped in the mining industry. They typically flow pseudo-homogeneously in turbulent pipe flow. The copper tails described by Thomas et al (1), and discussed later, is typical of such slurries.

To predict the flow behaviour of fine particle slurries in pipelines, rheology tests are conducted, usually in a rotational viscometer. A plot of the viscometer output parameters, shear stress and shear rate, represents the rheogram. When plotted on linear co-ordinates the rheogram generally exhibits a curved portion at low shear rates followed by a straight line portion at higher shear rates. The straight line fitted to the high shear rate data provides the Bingham parameters, yield stress and plastic viscosity. The Bingham model (2) shown in Equation 1 is one of the simplest and most convenient rheological models.

$$\tau_w = \tau_y + \eta_{pl}\,\gamma \qquad (1)$$

If the low shear rate, curved portion is applicable, then a three parameter model such as the Yield Power Law (Herschel Bulkley), (2) model may be fitted. The question is: When is the high shear rate straight line (Bingham) portion of the rheogram applicable and when is the low shear rate curved portion applicable, and how relevant is the curved portion anyway? Before we answer this we need to consider the relationship between laminar and turbulent pipe flow.

# 2 LAMINAR AND TURBULENT PIPE FLOW

## 2.1 Viscous sub-layer and shear rates in turbulent pipe flow

Consider turbulent flow in a smooth pipe. There is a thin, viscous sub-layer at the pipe wall within which the velocity profile is similar to that which would exist in laminar pipe flow. However, due to inertia effects, it becomes unstable a short distance from the wall and the mean velocity profile, instead of continuing with the laminar-like shape, breaks down to form the blunter turbulent velocity profile. Although the thickness of the viscous sub-layer is generally less than 1 mm, it nevertheless plays an important role in determining the turbulent velocity profile.

Within the viscous sub-layer the relationship between shear stress and shear rate is the same as in normal laminar flow. The wall shear stress applying to the turbulent flow conditions therefore determines the shear rate within the viscous sub-layer. Beyond the viscous sub-layer, the near-wall layers dominate the turbulent dissipation, Rudman et al (3), and shear rates are of similar order as in the viscous sub-layer. As a consequence, Rudman et al (3) quote Shook & Roco (4) as suggesting rheology measurements should be taken at least up to shear stress values (and consequent shear rates) corresponding to the mean wall shear stress in the turbulent flow of interest. As a result of their work, Rudman et al went even further, recommending rheology measurements should be conducted up to a maximum shear rate twice that applying at the turbulent flow mean wall shear rate. It will be shown in the next section how, for turbulent flow of a kaolin slurry in a specific pipe, this criterion would involve testing at shear rates up to around 14,000 $s^{-1}$. Although such high shear rates may be possible to achieve in a very small diameter tube viscometer, they are impossible to achieve in a rotational viscometer. The alternative is to fit a rheological model to the lower shear rate measured viscometer data which can be most confidently extrapolated to higher shear rates. Selection of such a rheological model represents a major part of this current paper.

## 2.2 Pipe flow data for kaolin slurry

Figure 1 shows wall shear stress ($\tau_w$= DJ/4) versus apparent shear rate (8V/D) for a 7.5% by volume, minus 23 μm, kaolin slurry in three pipe diameters, 105 mm, 18.9 mm, and 7.2 mm, (5). For any time–independent non-Newtonian fluid the laminar flow data from various pipe diameters should correlate on such a plot provided there is no wall slip, and this is seen to be the case for the kaolin slurry. The laminar flow data are shown transitioning to turbulent flow in the three pipe diameters at 8V/D=120 $s^{-1}$, 900 $s^{-1}$, and 2300 $s^{-1}$ respectively. The Buckingham equation (6), shown here as Eqn 2, describes the laminar flow behaviour in the three pipe diameters. At high values of $\tau_w$ (high 8V/D), the third term in the square brackets becomes small in magnitude compared to the second term, and at high enough values of 8V/D the third term can be ignored.

$$8V/D = \tau_w/\eta_{pl}\,[1 - 4/3(\tau_y/\tau_w) + 1/3\,(\tau_y/\tau_w)^4\,] \qquad (2)$$

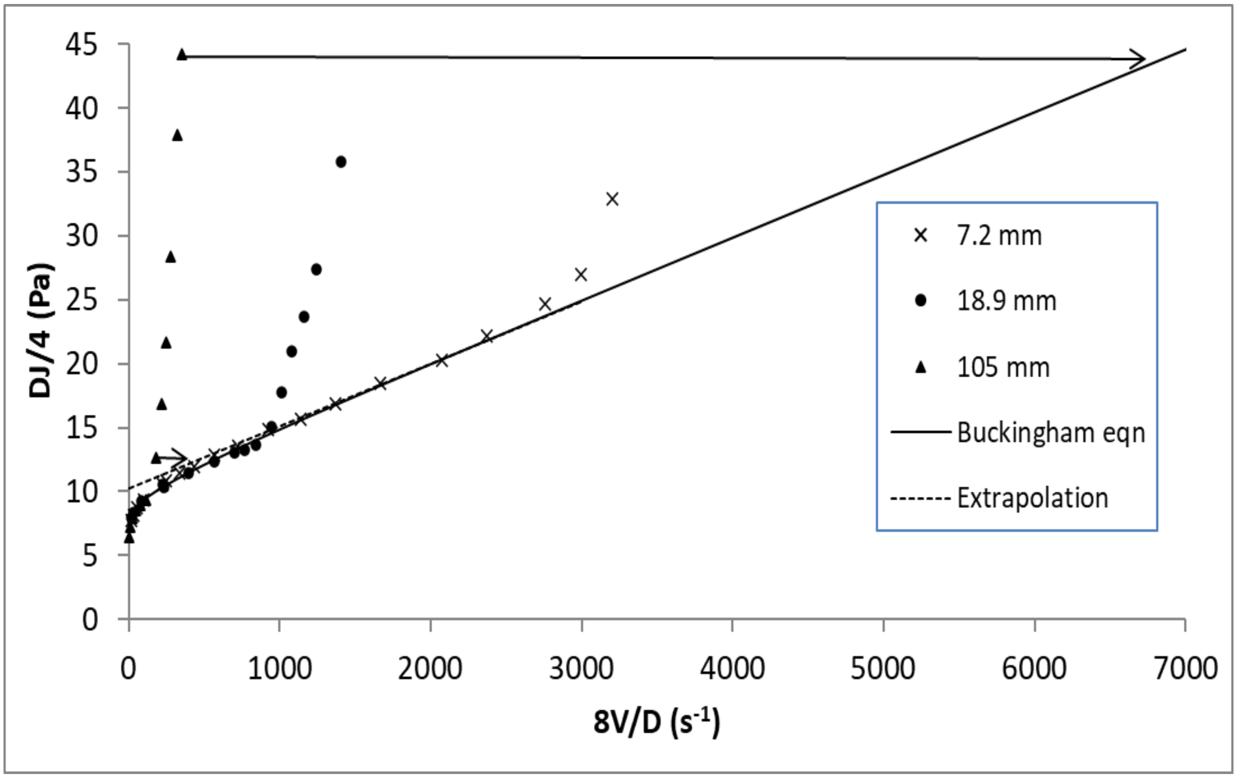


**Figure 1 Kaolin slurry in three pipe sizes. Wall shear stress versus Apparent Shear Rate, 8V/D from Thomas (5)**

As shown by the dashed line in Figure 1, an extrapolation of the 7.2 mm diameter tube, high shear rate (1150 $s^{-1}$ <8V/D< 2100 $s^{-1}$) laminar flow data, intersects the $\tau_w$ axis at 10.25 Pa, and if the third term is ignored, then the Bingham yield stress is equal to 3/4 of 10.25 Pa, i.e. 7.69 Pa, and the slope of the high shear rate data indicates a plastic viscosity of 0.0049 Pas. Note that for 8V/D less than about 1000 $s^{-1}$, the third term is more relevant and causes a pronounced curve in the data trend making it more difficult to determine the Bingham parameters from a straight line extrapolation.

The data, and the Buckingham equation prediction for $\tau_y$=7.69 Pa and $\eta_{pl}$=0.0049 Pas, curve down at very low shear rates because the slurry is not being sheared across the whole pipe diameter. Although not obvious in Figure 1, the data at the lowest shear rates fall slightly below the Buckingham prediction. The lowest measured wall shear stress, (in the 105 mm pipe at 0.014 m/s velocity, 8V/D=1.1 $s^{-1}$), is 6.44 Pa, which is 16% less than the 7.69 Pa Bingham model yield stress. This aspect is discussed in later sections in relation to rotational viscometers and in both cases the lower than predicted shear stress is probably due to wall slip (2). By chance, the lowest velocity in the 7.2 mm ID pipe is also 0.014 m/s (8V/D=16 $s^{-1}$) at a measured wall shear stress of 7.8 Pa.

Six turbulent flow data points are shown in Figure 1 for the 105 mm pipe. The lowest data point is DJ/4=12.6 Pa (8V/D=179 $s^{-1}$, V=2.35 m/s) and the highest is 44.2 Pa (8V/D=353 $s^{-1}$, V=4.63 m/s). It will be seen later in relation to rotational viscometry, how it is sometimes assumed that the operating 8V/D values in large pipes are indicative of the shear rates applying in turbulent flow. But this is far from the truth as indicated by the arrowed lines when the highest and lowest turbulent flow shear stresses in the 105 mm pipe (44.2 Pa and 12.6 Pa) are extended across to the laminar flow line. These give the actual shear rates in the viscous sub-layer based on the turbulent flow wall shear stress, as previously discussed in Section 2.1. At the highest turbulent flow wall shear stress of 44.2 Pa, the actual 8V/D equivalent shear rate in the viscous sub-layer is 6900 $s^{-1}$, rather than the apparent 8V/D=8x4.63/0.105=353 $s^{-1}$. At the lowest turbulent flow wall shear stress of 12.6 Pa, the actual 8V/D equivalent shear rate in the viscous sub-layer is 600 $s^{-1}$, rather than the apparent 8V/D=8x2.35/0.105=179 $s^{-1}$. This illustrates how selecting a region of a rheogram by assuming the shear rate applicable in turbulent flow will be similar to the 8V/D range calculated using the turbulent flow velocity, can cause large errors.

The above discussion involves the apparent shear rate (8V/D). The true shear rate, $\gamma$, can be obtained using the Rabinowitsch-Mooney equation (2), shown here as Eqn 3, by determining the slope, n', of a logarithmic plot of DJ/4 versus 8V/D.

$$\gamma = (3n' + 1)/(4\,n')\ 8V/D \qquad (3)$$

Applying Eqn 3 to the Buckingham equation fitted to the laminar flow data of Figure 1 with $\tau_y$=7.69 Pa and $\eta_{pl}$=0.0049 Pas, it is found that, for any particular wall shear stress, the true shear rate is approximately 500 $s^{-1}$ higher than the 8V/D equivalent shear rate.

# 3 ROTATIONAL VISCOMETRY

## 3.1 Introduction

In Section 2 it has been illustrated how laminar flow of a kaolin slurry in a 7.2 mm diameter pipe, which could be termed a tube viscometer, enabled the Bingham parameters to be determined. The alternative type of viscometer is a bob and cup rotational viscometer in which the slurry is sheared in the gap between a rotating cylindrical bob and a stationary cup. The gap is preferably small, only 1 or 2 mm, so that the shear rate is as high as possible and also so the shear rate across the gap can be considered approximately constant. The rotational viscometer requires a much smaller sample than the tube viscometer and is more convenient to use. Figure 2 shows some typical rheograms from rotational viscometer tests on a copper tails which were used in the design of a 1042 mm ID gravity flow tailings pipeline (1). The design analysis for this pipeline will be returned to in Section 4.2 in relation to turbulent flow pipeline design.

The viscometer used was a Contraves 115 with cup diameter 48.2 mm and bob diameter 45.6 mm, giving a gap of 1.3 mm. The shear rate is that quoted by the manufacturer which generally represents the shear rate at the mean diameter in the gap, i.e. (48.2+45.6)/2=46.9 mm. The highest shear rate quoted for this bob and cup combination is 661 $s^{-1}$ (7), which is consistent with that calculated as follows at the mean diameter of 46.9 mm, and at the highest 350 rpm rotational speed: $\gamma$=350/60 x $\pi$ 0.0469/0.0013=661 $s^{-1}$. The author is aware that there are more rigorous methods of calculating the shear rate, e.g. Krieger and Maron (8) and Cheng and Davis (9), which may give a slightly different result. However in this paper the more conventional shear rate quoted by the manufacturer is used, which has the advantage of not depending on the rheological property of the test fluid.

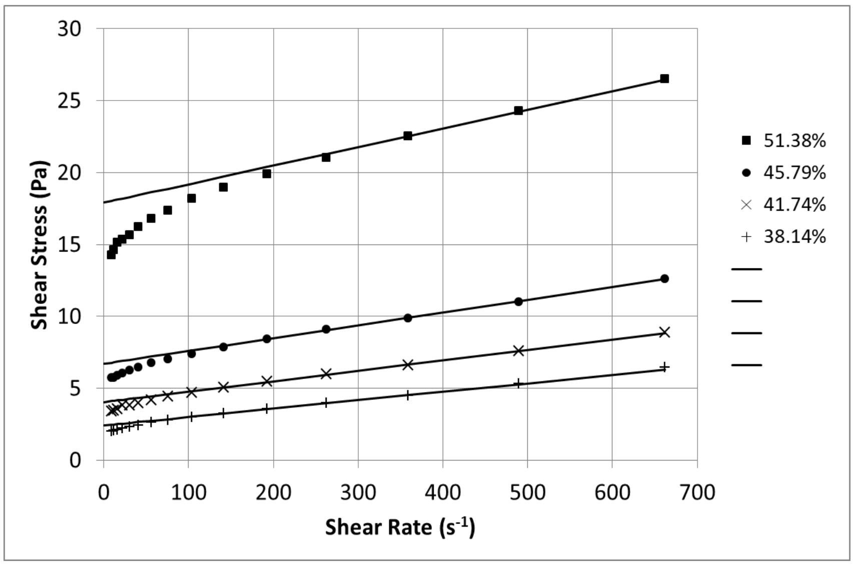


**Figure 2 Rotational viscometer rheograms for Sar Cheshmeh copper tails (1)**

The Figure 2 rheograms are shown for concentrations (w/w) ranging from Cw=38.14% to Cw=51.38%. Each data point represents the average of the ramp up and ramp down readings, which, for this particular, older, viscometer, are recorded manually. The speed is set at the lowest speed, the reading recorded, then the speed increased and recorded and so on. Once the maximum speed is recorded, rotation is stopped, the bob removed and the sample remixed with a spatula, then the bob replaced and ramp down begun. Ramp up and ramp down each take approximately 1½ minutes. For each concentration, the average difference between each of the 15 up and down readings is less than 1%, although the two lowest speed up and down readings vary by up to 3%.

Straight lines, representing the Bingham plastic model, have been fitted to the highest shear rate data points. Note how the data curve downwards at low shear rates in a similar manner as occurred with the kaolin pipe flow data of Figure 1. Just as was the case in the pipe flow of Figure 1, the curve downwards at low shear rates in Figure 2 is at least partly explained by the slurry not being fully sheared across the viscometer gap at low shear rates. This is analysed in Section 3.3. Note how the curved portion extends to higher shear rates as the concentration increases. At the highest concentration (Cw=51.38%), the curved portion extends to about 300 $s^{-1}$.

The highest shear rate with the Contraves 115 viscometer with this cup and bob combination, is 661 $s^{-1}$. This is higher than many commercial viscometers. Often a typical highest shear rate is around 500 $s^{-1}$. In addition, the diameter ratio bob/cup is typically lower than the 0.946 of the Contraves. The lower maximum shear rate and the lower ratio bob/cup diameter of most viscometers both mean that the curved portion of the rheogram will typically occupy a greater proportion of the rheogram than indicated in Figure 2. For example if the maximum shear rate in Figure 2 was only 500 $s^{-1}$ rather than 661 $s^{-1}$, the curved portion of the rheogram would occupy 2/3 of the shear rate range of the Cw=51.38% rheogram. With a more viscous slurry, almost the entire rheogram might have a curved shape. As a result, a Herschel Bulkley (Yield Power Law, YPL) model is sometimes fitted to the data (2) rather than a Bingham model. The dangers in this approach are discussed later in Sections 3.4 and 3.5.

### 3.2 Analysis of fully sheared viscometer flow of a Bingham plastic

It has been noted above how, as the shear rate decreases, for a slurry with a yield stress, eventually the slurry is not sheared across the whole gap, and this is, at least partly the explanation for the curve down in the data. First let us consider fully sheared flow of a Bingham plastic slurry.

The Reiner-Riwlin (6) equation is given below as Eqn 4.

$$\Omega = T/(4\pi h\eta_{pl})[1/R_b^2 - 1/R_c^2] - (\tau_y/\eta_{pl}) \operatorname{Ln}(R_c/R_b) \quad (4)$$

The torque, T, at the bob is given by Eqn 5 and the shear rate ($\gamma_b$) at the bob by Eqn 6.

$$T = 2\pi R_b^2 h\tau \quad (5)$$

$$\gamma_b = \Omega R_b/(R_c\text{-}R_b) \quad (6)$$

But the shear rate ($\gamma$) quoted by the viscometer manufacturers is the shear rate at the mean radius $(R_b+R_c)/2$. Therefore, in terms of mean shear rate, Eqn 6 becomes:

$$\gamma = \Omega(R_b+R_c)/2/(R_c\text{-}R_b) \quad (7)$$

i.e. $$\gamma = (R_b+R_c)/2/(R_c\text{-}R_b)[\tau R_b^2/2/\eta_{pl}(1/R_b^2\text{-}1/R_c^2) - \tau_y/\eta_{pl} \ln(R_c/R_b)] \quad (8)$$

or: $$\tau = 2\eta_{pl}/R_b^2/(1/R_b^2 - 1/R_c^2)[2\gamma(R_c\text{-}R_b)/(R_b+R_c) + \tau_y/\eta_{pl} \ln(R_c/R_b)] \quad (9)$$

Let us compare the equation for shear rate in a bob and cup rotational viscometer (Eqn 8), with the Buckingham equation for apparent shear rate in a tube (Eqn 2). There are only two terms in Eqn 8 with only one involving $\tau_y$. In contrast the second and third terms in Eqn 2 both involve $\tau_y$ with the third term involving the 4$^{th}$ power of $\tau_y$. The 4$^{th}$ power term results in significant curvature in the Buckingham plot, even at moderate shear rates. This means that high shear rate data are required in a tube viscometer to obtain the Bingham parameters from a straight-line extrapolation. In the case of the rotational viscometer, much lower shear rate data are sufficient for a straight-line extrapolation to obtain the Bingham parameters since there is no 4$^{th}$ power term in $\tau_y$ to cause a complicating curvature to the high shear rate portion of the rheogram. This is seen in the rotational viscometer data of Figure 2 where the maximum shear rate of 661 $s^{-1}$ is sufficient to provide the Bingham parameters for the highest Cw=51.38% for which $\tau_y$=16.8 Pa (see below), which is more than double the 7.69 Pa yield stress in Figure 1 which required true shear rates between 1650 $sec^{-1}$ to 2600 $s^{-1}$ to obtain the Bingham parameters from the straight-line extrapolation of the 7.2 mm pipe data.

Consider the Cw=51.38% data of Figure 2. A straight line fitted to the three highest data points and extrapolated, intercepts the shear stress axis at 17.75 Pa, i.e. $\tau_{ex}$=17.75 Pa. The line has a slope of 0.0132 Pas indicating $\eta_{ex}$=0.0132 Pas. For flow of a Bingham plastic in a pipe (Section 2.2), the extrapolated $\tau_{ex}$ was multiplied by ¾ to get the Bingham yield stress, $\tau_y$. For the present concentric cylinder case, according to (7) $\tau_{ex}$ is multiplied by $k_f$ to get $\tau_y$ where $k_f$ is given by Eqn 10. The current analysis finds that $\eta_{ex}$ should also be multiplied by $k_f$.

$$k_f = [1 - (R_b/R_c)^2] / [\ \ln (R_c/R_b)^2\ ] \quad (10)$$

In the present case where $R_b/R_c$=0.946, Eqn 10 gives $k_f$=0.947, which is essentially the same as 0.946. It is only when $R_b/R_c$ is less than about 0.85 that Eqn 10 gives a significantly different value than $R_b/R_c$. Hence for "narrow" gap viscometers, $k_f$ can be equated to $R_b/R_c$. In the present case, the Bingham parameters are therefore: $\tau_y$=0.946x17.75=16.8 Pa, and $\eta_{pl}$=0.946x0.0132=0.0125 Pas.

## 3.3 Analysis of partly sheared viscometer flow of a Bingham plastic

The Bingham parameters derived above for the Cw=51.38% data of Figure 2 are based on fitting a straight line to the three highest shear rate data points. The lower data points are ignored since it is assumed the downwards curve occurs because the slurry is not being fully sheared across the gap. Shearing then only occurs from the bob across part of the gap until the shear stress equals the yield stress. This is analogous to the situation in pipe flow as described by the Buckingham equation as shown in Figure 1. Defining $R_y$ as the radius at which the shear stress equals the Bingham yield stress, $\tau_y$, (e.g. 16.8 Pa for the Cw=51.38% slurry of Figure 3), $R_y$, for a Bingham plastic, is given (10 ) by Eqn 11.

$$R_y = R_b (\tau/\tau_y)^{0.5} \quad (11)$$

For any given $\tau$, $R_y$ is calculated. If $R_y > R_c$ then Eqn 8 is used to predict $\gamma$. As the shear stress is reduced, eventually $R_y$ becomes equal to $R_c$. From Eqn 11 this critical shear stress occurs when $\tau = \tau_y/0.946^2$. Once $R_y < R_c$ then Eqn 8 is used with $R_y$ substituted for $R_c$. The two-part, straight line in Figure 3 shows the result. Below the critical shear rate, shearing does not occur over the whole gap and the predicted Bingham behavior follows a straight line of steeper slope as indicated in Figure 3. However the measured data follow a significantly lower path than that predicted for the Bingham plastic with $\tau_y$=16.8 Pa. For example, the lowest measured data point (14.2 Pa at 8.88 $s^{-1}$) is 15% lower than the Bingham yield stress. (This difference is comparable with the 16% lower measured shear stress noted in relation to the Buckingham equation prediction in Figure 1). Part of the reason for the low measured values may be due to wall slip (2) at the bob surface at low shear rates. Slippage is known to sometimes occur and in recent years vane shaped bobs have been proposed to minimise slippage. Another explanation may be reduced solids concentration within the gap as some particles settle out under sheared conditions. If these possibilities are ignored and the curve-down behaviour is considered an inherent property of the slurry, a YPL curve may be fitted as shown in Figure 3. The consequences of this are discussed in Sections 3.4 and 3.5 below.

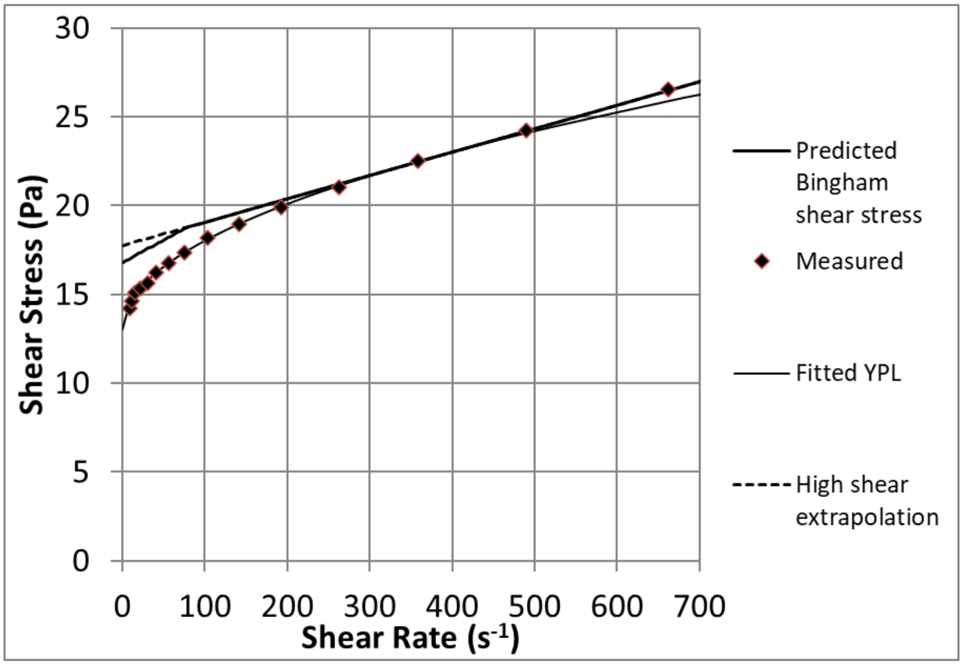


**Figure 3 Predicted Bingham shear stress and fitted YPL – Sar Cheshmeh 51.38%**

The two-part Bingham prediction line for shear stress in the rotational viscometer in Figure 3 was obtained using Eqn 8. However it can simply be constructed on the rheogram as follows: From Eqn 11, the critical shear stress at which the line slope changes, is given by Eqn 12.

$$\tau_{crit} = \tau_y /(R_b/R_c)^2 \qquad (12)$$

The critical shear rate at which the line slope changes, lies on the line $\tau = \tau_{ex}+\eta_{ex}\gamma$ and so:

$$\gamma_{crit} = (\tau_{crit} - \tau_{ex})/\eta_{ex} \qquad (13)$$

In the present case where $R_b/R_c$=0.946, extrapolation of the straight line fitted to the three highest data points gives $\tau_{ex}$=17.75 Pa and $\eta_{ex}$=0.0132 Pas and this gives the high shear rate portion of the two-part Bingham prediction line. Multiplying both by 0.946 gives $\tau_y$=16.8 Pa and $\eta_{pl}$=0.0125 Pas. Therefore from Eqn 12, $\tau_{crit}$=18.8 Pa and from Eqn 13, $\gamma_{crit}$=79.5 $s^{-1}$. A straight line from this critical point (79.5,18.8) to the yield stress at zero shear rate (0,16.8) completes the two-part Bingham prediction line for $\tau_y$=16.8 Pa and $\eta_{pl}$=0.0125 Pas.

So by fitting a straight line to the high shear rate data of the Cw=51.38% rheogram in Section 3.2, we have obtained the Bingham parameters $\tau_y$ and $\eta_{pl}$. Reversing the procedure, by inserting the determined $\tau_y$ and $\eta_{pl}$ values into Eqn 8 or 9, we can predict the high shear rate portion of the two-part Bingham prediction. Then, in this Section, Eqns 12 and 13, have been used to construct the low shear rate portion of the two-part Bingham prediction. Knowing $\tau_y$ and $\eta_{pl}$ for any slurry we can therefore obtain the two-part Bingham prediction line for flow of the 51.38% slurry in a rotational viscometer of different geometry (although this will not normally be required). This is analogous to determining the Bingham parameters from the 7.2 mm pipe diameter kaolin data of Figure 1 and then using the Buckingham equation (Eqn 2) to predict laminar Bingham behaviour in any size pipe knowing $\tau_y$ and $\eta_{pl}$. In both cases the predictions allow for part shearing at low shear rates but the measured data are lower than the low shear rate prediction with the lowest data point being 16% lower than the Bingham yield stress in Figure 1 and 15% lower in Figure 3.

## 3.4 Consequences for laminar pipe flow pressure gradient prediction

Although the two-part Bingham prediction in Figure 3 predicts higher than measured shear stress in the low shear rate region, it does illustrate an important point since it indicates that at least some of the curve-down behavior of the low shear rate data is because the slurry is not being sheared across the whole gap. Without this knowledge, some workers might fit a Yield Power Law (YPL) model to the low shear rate measured data as indicated in Figure 3, in the belief that all of the curve-down data represents an inherent property of the slurry. Note that Wasp et al (11) state categorically that the curved portion occurs purely because the slurry is not being sheared across the complete gap and that a rheological model (e.g. YPL) should not be fitted to the curved portion data. Slatter and Wasp (11) also argue in favour of the Bingham model rather than the YPL model.

A YPL model fitted to the curve-down data cannot be entirely accurate if some of the curve-down behaviour is because the slurry is not being sheared across the full gap or is due to other factors. If these "incorrect" YPL model parameters are used to predict laminar flow in a pipe, they will under-predict the pressure gradient. It may be better to use the Bingham model which may over-predict the pressure gradient thereby providing an in-built safety margin. Of course, to use a Bingham model, there has to be some straight line data at high shear rates to fit a straight line to. If a particular viscometer is limited in maximum shear rate, the most viscous slurry to which a Bingham model can be fitted will also be limited. For example, if the maximum shear rate of a particular viscometer is only 300 $s^{-1}$, it would be difficult to fit a straight line to the highest shear rate data of the Cw=51.38% slurry of Figure 3. If a straight line were fitted, it would give a lower yield stress and higher plastic viscosity than the line shown. With a 300 $s^{-1}$ maximum shear rate, determination of the Bingham parameters of the slurry of Figure 3 would be limited to a maximum concentration of about Cw=41.74%. (See Figure 2).

## 3.5 Consequences for turbulent pipe flow pressure gradient prediction

The above comments apply to laminar pipe flow prediction. Use of the "incorrect" YPL parameters may also result in errors in turbulent flow prediction. This is illustrated in Figure 4, which shows extrapolation of the Bingham and the fitted YPL models of Figure 3 out to a shear rate of 7000 $s^{-1}$. It was discussed in Section 2.1 how, for one particular turbulent pipe flow prediction, rheology data to 7000 $s^{-1}$, or even twice this, was ideally needed. The fitted YPL in Figure 4 predicts a shear stress at 7000 $s^{-1}$ of about half that predicted by the Bingham model fitted to the high shear rate data of Figure 3. i.e. the effective viscosity ($\tau_w/\gamma$) at 7000 $s^{-1}$ based on the YPL fit, is about half the effective viscosity based on the Bingham model. Although not shown in Figure 4, at 14000 $s^{-1}$ the YPL prediction is only 35% of the Bingham prediction. These differences between the Bingham and YPL effective viscosities at very high shear rates will have a significant effect on turbulent flow prediction. With some slurries, a YPL model fitted to viscometer data can predict effective viscosities less than water at high shear rates, which would seem absurd. In contrast, as shear rate increases, the effective viscosity when using the Bingham model tends towards a Newtonian fluid with viscosity equal to the plastic viscosity.

For these reasons the author believes the Bingham model is preferred for turbulent flow prediction, even though the low shear rate rotational viscometer data may deviate from the two-part Bingham prediction as seen in Figure 3. That this deviation does not matter is supported by the following three papers in chronological order. Firstly, Slatter and Wasp (12) after considering a number of criteria, concluded that it could be assumed that rheometric data below a certain shear rate are relatively unimportant for the (turbulent) pipe flow problem. Secondly, Wilson and Thomas (13) came to a similar conclusion after extending their non-Newtonian, turbulent flow prediction to a hybrid, cubic-spline-Bingham rheological model which in some cases fitted the curve-down behavior at low shear rates. Such a hybrid model followed the low shear rate curved data to some extent before merging into the Bingham model at higher shear rates. They showed that turbulent flow predictions using the hybrid model were little different from predictions using the pure Bingham model which ignored the curve-down data. The reason is because there is negligible difference in the area under the two curves when extended to the high shear rates applicable in turbulent flow, such as in Figure 4. They concluded that for turbulent flow prediction, the low shear rate curved data can be ignored and a Bingham model fitted to the high shear rate data can be used. Thirdly, a recent Direct Numerical Simulation (DNS) study (3) found that accurate rheology measurement (or extrapolation) is absolutely essential at high shear rates for turbulent flow prediction whereas low shear rate data was probably less important. These three papers together provide strong justification for the use of the Bingham model rather than the YPL model for turbulent flow prediction.

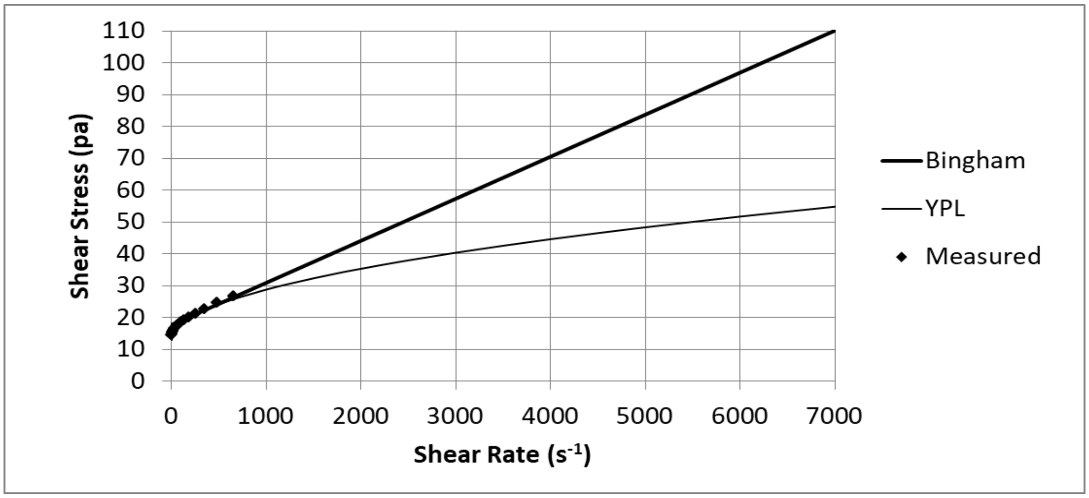


**Figure 4 Bingham and YPL extrapolations to 7000 s$^{-1}$ – Sar Cheshmeh 51.38%**

### 3.6 Other Viscometers

The rotational viscometer data discussed above were obtained using a Contraves 115 viscometer in which the shear rates steps are a geometric progression. On a linear plot this means the majority of the data points are at the lower shear rate end. Older viscometers, such as this Contraves, tended to be set up with geometric progressions. In contrast, with modern viscometers, most workers select an arithmetic progression, which evenly distributes the data on a linear plot. The effect of the differences is illustrated in Figure 5 which compares the Sar Cheshmeh copper tails rheogram of Figure 3 (Cw=51.38%) with recent data obtained with Slurry Systems' modern viscometer on a zinc tails with a rather similar rheology. The same bob and cup are used in both viscometers. The Bingham straight lines fitted to the high shear rate data are based on the following extrapolated values: Sar Cheshmeh copper tails, $\tau_{ex}$=17.75 Pa, $\eta_{ex}$=13.2 mPas: Zinc tails, $\tau_{ex}$=15.2 Pa, $\eta_{ex}$=14.3 mPas.

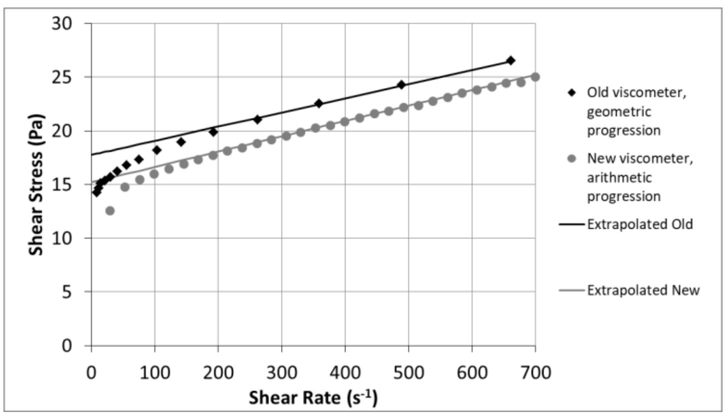


**Figure 5 Comparison viscometer data with geometric and arithmetic progressions**

Of the 15 data points from the old viscometer in Figure 5, only three are used for the Bingham model fit with 12 in the low shear rate curved portion below 300 s$^{-1}$. i.e. 80% of the data points are in the curved portion of the rheogram. In contrast the new viscometer has 30 data points, with 22 used for the Bingham model and only 8 in the low shear rate curved portion below 200 s$^{-1}$. i.e. only 27% of the data points are in the curved portion of the rheogram. These comparisons illustrate how, even purely from a psychological viewpoint, the geometric progression used in most older type viscometers tends to encourage the fitting of models such as the YPL to the lower shear rate data. In contrast, the arithmetic progression mostly selected in the newer viscometers, tends to encourage the fitting of a Bingham model to the high shear rate data. The author has noticed that workers in various groups in earlier years often tended to apply the YPL model rather than the Bingham model but that with more modern viscometers, the Bingham model is now being applied more often.

# 4 ROTATIONAL VISCOMETER DATA USE IN PIPELINE DESIGN

## 4.1 Laminar flow pipeline design using rotational viscometer data

Following the work of Thomas (14), Gillies at al (15), Cooke (16) and others, it is now generally accepted that in most cases, to achieve equilibrium laminar flow in a long pipeline without a stationary bed forming, the pressure gradient needs to be roughly greater than about 2 kPa/m. (For solid density 2.65 $t/m^3$). The only exception would be a slurry composed of all colloidal sized particles such as pure kaolin for example. Pipelines transporting part colloidal slurries, have operated in laminar flow by allowing for a slow bed build-up with regular flushing or pigging every few days for example (17). Nevertheless there is often a strong incentive to pump at as high a concentration as possible to minimise water consumption, meaning that laminar flow operation is required. The use of rotational viscometer data for laminar flow pipeline design will now be illustrated in relation to the rheogram of Figure 6 which applies to a minus 0.125 mm tails primarily consisting of clays, mainly kaolin, with some quartz. The average solids density is 2.5 $t/m^3$. The rheogram was obtained in the same Contraves viscometer as in previous figures but with a modified B system cup and bob with $R_c$=16.25 mm and $R_b$=15 mm, giving a gap of 1.25 mm and $R_b/R_c$=0.9231.

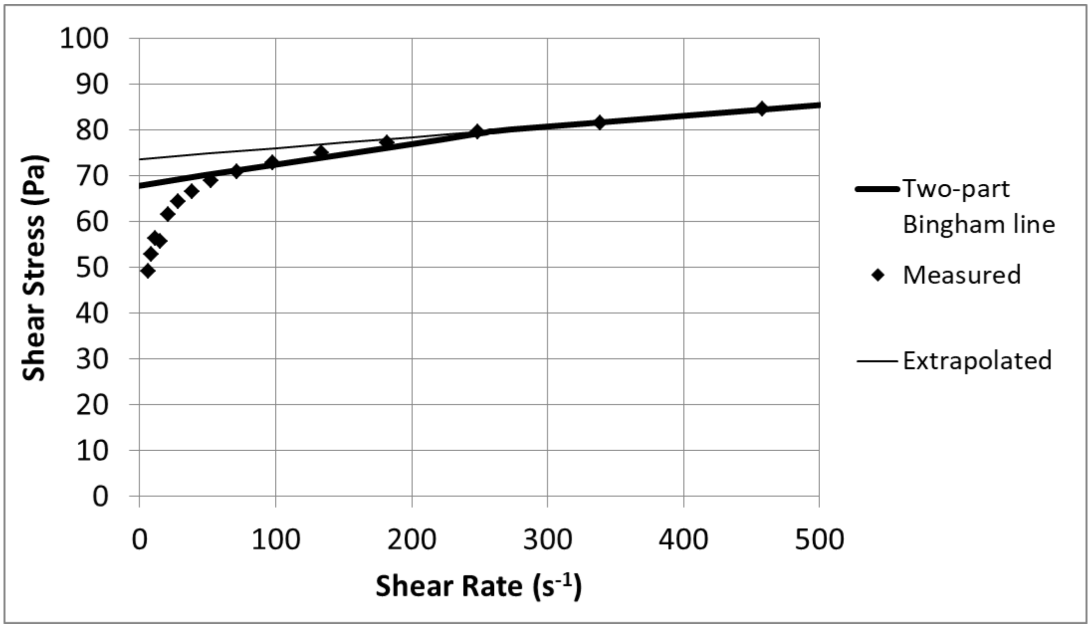


**Figure 6 Minus 0.125 mm tails rheogram, Cw=25.22%**

A straight line drawn through the three highest data points extrapolated to the shear stress axis gives $\tau_{ex}$=73.6 Pa and $\eta_{ex}$=0.0240 Pas, and this represents the high shear rate portion of the two-part Bingham prediction line for the shear stress in the viscometer. Multiplying both by 0.9231 gives $\tau_y$=67.9 Pa and $\eta_{pl}$=0.022 Pas. Therefore from Eqn 12, $\tau_{crit}$=79.7 Pa and from Eqn 13, $\gamma_{crit}$=253 $s^{-1}$. A straight line from this critical point (253.5,79.68) to the yield stress at zero shear rate (0,67.9) completes the two-part Bingham prediction line for $\tau_y$=67.9 Pa and $\eta_{pl}$=0.022 Pas. The two-part prediction line adequately describes the data down to about 50 $s^{-1}$ shear rate. The next step is to use the Bingham parameters to predict pipe flow using the Buckingham equation (2).

According to Wilson and Thomas (18), the transition velocity, $V_t$, between laminar and turbulent pipe flow of a Bingham plastic is given by Eqn 14. Slatter and Wasp (19) gave a similar equation with the constant 26. The $\tau_y$ in Eqn 14 is the Bingham yield stress, not a measured static yield stress. Note that Eqn 14 is independent of pipe diameter.

$$V_t = 25(\tau_y/\rho_{sl})^{0.5} \qquad (14)$$

For the Cw=25.22% slurry of Figure 6 with $\tau_y$=67.9 Pa and $\rho_{sl}$=1178 $kg/m^3$, $V_t$=6.0 m/s meaning that turbulent flow operation would require a velocity around 7 m/s. It is unlikely that such a high velocity would be considered because of pipe wear considerations. Therefore laminar flow operation is now analysed.

As noted above, the rule of thumb minimum pressure gradient required for laminar flow operation is 2 kPa/m for solids density 2.65 $t/m^3$. Based on relative density in water this translates to 1.5/1.65x2=1.82 kPa/m for solids density 2.5 $t/m^3$. The tailings are to be pumped over level terrain a distance of 800 m to a tailings dam. A 200 OD PE100 PN25 HDPE pipe is selected with ID 143 mm. A design velocity of 3 m/s is selected with 2 m/s minimum operating velocity. At 3 m/s velocity the Buckingham equation (Eqn 2) gives a laminar flow pressure gradient of 2.265 kPa/m (1812 kPa over 800 m), and at 2 m/s Eqn 2 gives 2.19 kPa/m (1752 kPa over 800 m).

At the minimum 2 m/s velocity, the 2.19 kPa/m pressure gradient exceeds the minimum required 1.82 kPa/m pressure gradient by 20% indicating that steady equilibrium laminar flow should be achieved in the pipeline. The maximum pipeline pressure is 1812 kPa which is comfortably below the 2500 kPa maximum pressure for PN25 HDPE pipe.

Note that over the velocity range 2 m/s to 3 m/s, the apparent shear rate (8V/D) ranges from 112 $s^{-1}$ to 168 $s^{-1}$. If equated to the true shear rate, these 8V/D values are within the Figure 6 data range which is described by the two-part Bingham prediction so the Buckingham pipe flow prediction is applicable. Using Eqn 3, the actual true shear rate at 3 m/s is 580 $sec^{-1}$ and at 2 m/s is 462 $sec^{-1}$. These true shear rates are within the upper portion of the two-part Bingham prediction line in Figure 6 so the Bingham prediction is once again applicable.

### 4.2 Turbulent flow pipeline design using rotational viscometer data

It was shown in Section 3.5 how the fitting of a YPL model to the curve-down low shear rate data of a rheogram, can result in low effective viscosities at the very high shear rates applicable in turbulent flow. However it will be shown in this section that generally, for a narrow gap viscometer, the requirements for turbulent pipe flow mean that only data in the non-curved region of the rheogram is applicable anyway.

Figure 7 is a plot of the three lower concentration data of Figure 2. The data were used in the design of the 1042 mm ID Sar Cheshmeh gravity flow copper tailings pipeline in Iran, as described by Thomas et al (1). The particle sizing is: $d_{50}$=40 μm, $d_{80}$=120 μm and $d_{99}$=280 μm. The solids density is 2.8 $t/m^3$. The three concentrations shown are essentially the maximum, nominal and minimum design concentrations. Also shown in Figure 7 are the two-part Bingham predictions for the shear stress in the rotational viscometer as per Sections 3.2 and 3.3, based on the following Bingham parameters:

Maximum Cw=45.79%: $\tau_y$=6.34 Pa, $\eta_{pl}$=8.45 mPas
Design Cw=41.74%. $\tau_y$=3.82 Pa, $\eta_{pl}$=6.82 mPas
Minimum Cw=38.14%: $\tau_y$=2.28 Pa, $\eta_{pl}$=5.54 mPas

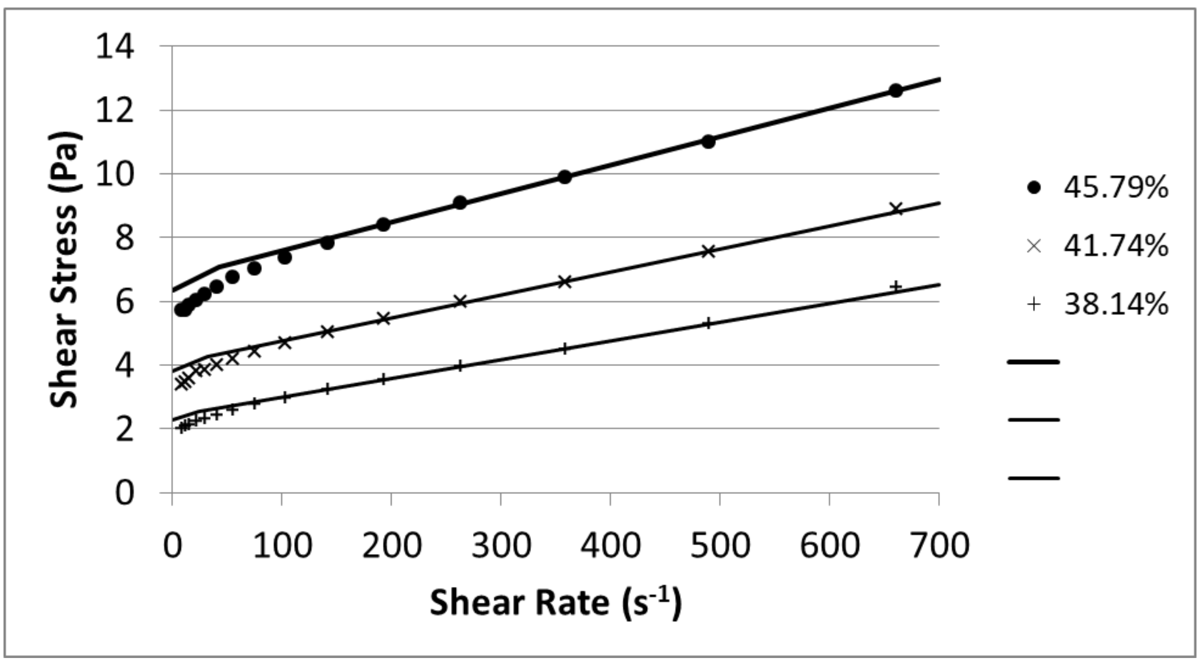


**Figure 7 Measured rheogram data of the three lower concentrations of Figure 2 together with two-part Bingham predictions for shear stress in the viscometer**

The Operating Envelope given in (1) for the 1042 mm ID pipeline shows that the pipeline operating flow rate at Cw=41.74% ranges from 9400 $m^3$/h set by the maximum available (gravity) head to 5000 $m^3$/h set by the need to operate a safe margin above the laminar/turbulent transition velocity. This flow rate range equates to velocities of 3.06 m/s to 1.63 m/s, with the lower velocity a safe 0.27 m/s margin above the laminar/turbulent transition velocity, which from Eqn 14 is 1.36 m/s.

Based on the prediction method of Wilson and Thomas (20) and its inclusion of pipe roughness by Thomas and Wilson (21), the predicted turbulent flow pressure gradient (J) in the steel pipe (roughness 0.05 mm) for Cw=41.74% at 3.06 m/s is 73.0 Pa/m. The wall shear stress ($\tau_w$) equals DJ/4 = 1.042x73/4 = 19.0 Pa which, from Figure 7, is obviously off the graph in the extrapolated straight line portion of the rheogram. The relevant shear rate (γ) can be found using the Bingham equation (1) to be 2225 $s^{-1}$. At the minimum 1.63 m/s operating velocity, J=19.8 Pa/m and the wall shear stress $\tau_w$ equals 5.16 Pa. The relevant shear rate (γ) can be found using the

Bingham equation (1) to be 196 $s^{-1}$. It is seen in Figure 7 that the straight line Bingham fit for Cw=41.74% is relevant at $\tau_w$ =5.16 Pa and $\gamma$ =196 $s^{-1}$. As discussed in Section 3.5, as long as the wall shear stress in turbulent flow is in the straight line portion of the rheogram, the fact that there is the curved region at low shear rates was shown by Wilson and Thomas (13) to have negligible effect on the predicted turbulent flow Bingham behaviour. Summarising, for Cw=41.74% the Bingham straight line fit is relevant to the operating velocity range between 3.06 m/s and 1.63 m/s.

Similar conclusions are obtained for the other two concentrations in Figure 7. For Cw=45.79% the relevant operating shear rate ranges from maximum of about 1500 $s^{-1}$ to minimum of about 75 $s^{-1}$. For Cw=38.14% the relevant operating shear rate ranges from a maximum of 2965 $s^{-1}$ to a minimum of 490 $sec^{-1}$. Thus for both concentrations the straight line Bingham model essentially covers the turbulent shear rate range. Note that at the lowest design concentration, Cw=38.14%, the lower velocity limit (1.30 m/s) is dictated by turbulent deposition rather than transition. Turbulent deposition prediction procedures for Bingham plastic slurries have been recently described by Thomas (22).

The above example applies to a 1042 mm ID pipe which is larger than typical. Applying the same analysis for this slurry to a smaller pipe, shows that for the same velocity range the wall shear stress is even more relevant to the straight line portions of the rheograms. For example in a 200 mm ID pipe for Cw=41.74% the predicted wall shear stresses are:

At V=3.06 m/s, J=541 Pa/m, DJ/4=27.0 Pa c.f. only 19 Pa in the 1042 ID pipe
At V=1.63 m/s, J=141 Pa/m, DJ/4=7.05 Pa c.f. only 5.16 Pa in the 1042 ID pipe

## 4.3 Particle size effects in rotational viscometry

The current work has emphasised the advantages of rotational viscometers with as high shear rates as possible. High shear rates require a small gap between the bob and cup which necessarily limits the maximum particle size of the slurry. For a slurry with a narrow particle size distribution a common recommendation is that the maximum particle size should be limited to about 1/10th of the gap between the bob and cup. In the case of the typical gap discussed in the present paper, 1.30 mm, this would limit the maximum particle size to less than 0.13 mm. However, apart from beach sands, most industrial slurries do not have a narrow size distribution. Slurries which are formed by comminution generally have quite wide size distributions. For such slurries, in the author's experience, screening at 0.85 mm or 0.60 mm, is generally sufficient with a 1.30 mm gap viscometer.

Once some particles are excluded from testing in the viscometer, a means of adjusting the measured rheology for the effect of the excluded coarser particles is required. Excluded particles greater than 0.60 mm for example, when recombined with the tested slurry, will increase the measured rheology in a purely mechanical manner as described for example in (23) and (24) which give examples of how the measured rheology of the say minus 0.60 mm slurry can be adjusted to take into account the excluded plus 0.60 mm particles. The same approach can be used if only say the minus 75 μm slurry is tested.

There is an interesting aside regarding exclusion of coarse particles from testing in the viscometer. In turbulent pipe flow, particles which are coarser than the viscous sub-layer cannot influence the viscosity in the wall region. This was illustrated (25) by the differing behaviour of two sands in water in turbulent pipe flow when pressure gradient is plotted against velocity on a log-log plot. At very high velocities the pressure gradient of a 1.2 mm sand slurry approached the pressure gradient of water whereas the pressure gradient of a 0.13 mm sand slurry plotted above and parallel to the water pressure gradient. This differing behaviour is commonly seen in Durand type (26) plots. The 1.2 mm sand is too coarse to fit in the sub-layer and is effectively transported with no additional energy requirement. In contrast the 0.13 mm sand can fit into the sub-layer and increase the viscosity, and hence increases the pressure gradient. For fluid viscosities between 5 and 10 mPas (27) predicted sand particle sizes greater than about 0.4 mm to 0.8 mm were too large to influence the sub-layer viscosity. These fluid vicosities are of similar order to the plastic viscosities of Figure 7 for example. So in some respects this might suggest that there is no need to adjust the measured rheology for excluded particles of size 0.4 mm to 0.8 mm when using the measured data to predict turbulent flow behaviour..

## 5 CONCLUSIONS

It has been shown how very high shear rate rheological data is required for accurate turbulent pipe flow prediction. Since rotational bob and cup viscometers are necessarily limited to quite low shear rates, any rheological model fitted to the viscometer data should be robust enough to permit accurate extrapolation to very high shear rates. Typically the rheogram data follow a straight line at high shear rates followed by down-curve data at low shear rates. The down-curve behaviour is at least partly due to the slurry being only part sheared and therefore cannot be considered an inherent property of the slurry. Only the straight-line high shear rate data is relevant, and a Bingham model fitted to this data is recommended. A method of determining the Bingham parameters and predicting the viscometer behaviour with allowance for part shearing at low shear rates, has been presented. The use of a Yield Power Law (YPL) model fitted to the low shear rate, down-curve data, is not recommended, even for low shear rate laminar flow prediction.

## 6 REFERENCES


1 Thomas, A.D. , Rieschiek, R. and Roshdieh, A. (2017), Design of the Sar Cheshmeh gravity flow tailings pipeline, Iran, Hydrotransport 20 Conf., Melbourne, Australia, 3-5 May 2017.

2 Brown, N.P. and Heywood, N.I. (1991), Slurry Handling, Design of Solid-liquid Systems, Elsevier.

3 Rudman, M., Singh, J., Blackburn, H.M., Chryss, A., Graham, L.J. and Pullum, L. (2015), The importance of rheology shear rate for DNS of turbulent flow of yield stress fluids, 17th Int. Conf. on Transport and Sedimentation of Solid Particles, Delft, The Netherlands, 22-25 Sept 2015.

4 Shook, C.A. and Roco, M.C. (1991). Slurry Flows: Principles and Practice, p81, Butterworth – Heinemann.

5 Thomas, A.D. (1981) Slurry Pipeline Rheology, Keynote Lecture, 2nd National Conf. on Rheology, Sydney, Australia, 14-15 May, 1981.

6 Abulnaga, B.E. (2002), Slurry Systems Handbook, McGraw-Hill

7 Contraves 115 Manual (1980), Measurement of rheological properties. Contraves AG, Zurich.

8 Krieger, I.M. and Maron, S.H. (1954), *J. Appl. Phys,* ***25****, 72*.

9 Cheng, D.C-H. and Davis, J.B. (1969), Rheol. Acta, 8, 161-173

10 Bird, R.B., Stewart, W.E. and Lightfoot, E.N. (1960), Transport Phenomena, John Wiley & Sons

11 Wasp, E.J., Kenny, J.P. and Gandhi, R.L. (1977), Solid-Liquid Flow, Slurry Pipeline Transportation, TransTech Publications, Clausthal, Germany.

12 Slatter, P.T. and Wasp, E.J. (2002). The Bingham plastic rheological model: friend or foe? Hydrotransport 15 Conf., Banff, Canada, 3-5 June 2002.

13 Wilson, K.C. and Thomas, A.D. (2008), Hybrid rheological model for predicting non-Newtonian turbulent pipe flow, 14th Int. Conf. on Transport and Sedimentation of Solid Particles, St Petersburg, Russia, 23-27 June 2008.

14 Thomas, A.D. (1979). Pipelining of Coarse Coal as a Stabilized Slurry – Another Viewpoint, 4th Int. Tech. Conf. on Slurry Transportation, Las Vegas, 28-30 March, 1979.

15 Gillies, R.G., Hill, K.B., McKibben, M.J. and Shook, C.A. (1999). Solids transport by laminar Newtonian flows, Powder Technology **104** 269-277.

16 Cooke, R. (2002). Laminar flow settling: the potential for unexpected problems, Hydrotransport 15 Conf., Banff, Canada, 3-5 June 2002.

17 Wasp, E.J. (1999). Instability of laminar flow in long distance pipelines. Rheology in the Mineral Industry II, Engineering Foundation (USA) International Conference, Hawaii

18 Wilson, K.C. and Thomas, A.D. (2006), Analytic model of laminar-turbulent transition for Bingham plastics, Can. J. Chem. Eng., Oct 2006.

19 Slatter, P.T. and Wasp, E.J. (2000), The laminar /turbulent transition in large pipes, 10th Int. Conf. on Transport and Sedimentation of Solid Particles, Wroclaw, Poland, 4-7 September 2000.

20 Wilson, K.C and Thomas, A.D. (1985). A new analysis of the turbulent flow of non-Newtonian fluids, Can. Jnl Chem. Engnr, Vol. 63, August 1985.

21 Thomas, A.D. and Wilson, K.C. (2007), Rough-wall and turbulent transition analyses for Bingham plastics, Hydrotransport 17 Conf., Capetown, South Africa, 7-11 May 2007.

22 Thomas, A.D. (2019). Deposition of wide size distribution, Bingham plastic slurries in turbulent pipe flow. 19th Int. Conf. on Transport and Sedimentation of Solid Particles, Capetown, South Africa, 24-27 September 2019.

23 Thomas, A.D. (1999). The Influence of Coarse Particles on the Rheology of Fine Particle Slurries, Rheology in the Mineral Industry II, United Engineering Foundation Conference, Turtle Bay, Hawaii, March 1999.

24 Thomas, A.D.(2010). Method of determining the inherent viscosity of a slurry and other rheological trends as illustrated by a data bank of over 200 different slurries. Hydrotransport 18 Conf., Rio de Janeiro, Brazil, 22-24 September.

25 Thomas, A.D. (1977). Particle Size Effects in Turbulent Pipe Flow of Solid-Liquid Suspensions, 6th Australasian Hydraulics and Fluid mechanics Conference, Adelaide, 5-9 December 1977.

26 Durand, R. (1953). Basic relationship of the transportation of solids in experimental research. Proc. Of the International Association for Hydraulic Research-University of Minnesota, September 1953.

27 Thomas, A.D. (1978). Coarse Particles in a Heavy Medium – Turbulent Pressure Drop Reduction and Deposition under Laminar Flow, Hydrotransport 5 Conf., Hannover, 8-11 May, 1978.